Calcification depths of planktic foraminifers constrained by geochemical signatures from sediment-trap samples from the Bay of Bengal

Ayumi Maeda[1], Azumi Kuroyanagi[2], Toshihiro Yoshimura[3], Birgit Gaye[4], Tim Rixen[5], Atsushi Suzuki[1], Hiroshi Nishi[2,6] and Hodaka Kawahata[7]

[1] Geological Survey of Japan, National Institute of Advanced Industrial Science and Technology, 1-1-1 Higashi, Tsukuba, Ibaraki 305-8567, Japan.

[2] Tohoku University Museum, Tohoku University, 6-3 Aoba, Aramaki, Aoba-ku, Sendai 980-8578, Japan.

[3] Japan Agency for Marine-Earth Science and Technology, 2-15 Natsushimacho, Yokosuka, Kanagawa 237-0061, Japan.

[4] Institute for Geology, Universität Hamburg, Bundesstraße 55, D-20146 Hamburg.

[5] Leibniz Centre for Tropical Marine Research (ZMT), Fahrenheitstrasse 6, D-28359 Bremen.

[6] Institute of Dinosaur Research, Fukui Prefectural University, Matsuo kakenjojima 4-1-1, Yoshida-gun Eiheijicho, Fukui 910-1142, Japan.

[7] Atmosphere and Ocean Research Institute, The University of Tokyo, 5-1-5 Kashiwanoha, Kashiwa-shi, Chiba 277-8564, Japan

Corresponding author: Ayumi Maeda (ay-maeda@aist.go.jp)

Key Points:

- The apparent calcification depths were obtained using planktic foraminifers from sediment trap samples moored in the Bay of Bengal.
- *G. ruber* reflects the temperature within the mixed layer, whereas *N. dutertrei* in the upper thermocline and *T. sacculifer* between them.
- The flux-weighted values of $\delta^{18}O$ of a species correspond to the mean annual $\delta^{18}O$ value of that species.

Abstract

The Mg/Ca and oxygen isotope ratios ($\delta^{18}O$) of multiple species of planktic foraminifers provide information on the hydrological conditions between the surface and the thermocline. Knowledge of the apparent calcification depth (ACD) of planktic foraminifers is key to reconstructing paleoenvironments; however, ACDs exhibit seasonal variations and differ over regional scales. We obtained the ACDs of *Globigerinoides ruber*, *Trilobatus sacculifer*, and *Neogloboquadrina dutertrei* in the Bay of Bengal using multiyear sediment-trap samples collected at approximately 900 m depth. The sediment traps were moored in the southwestern Bay of Bengal, with sampling intervals of 17–42 days. The temperature estimates obtained from the $\delta^{18}O$ and Mg/Ca patterns of *G. ruber*, *T. sacculifer*, and *N. dutertrei* indicate that *G. ruber* reflects the temperature within the mixed layer, whereas *N. dutertrei* precipitates its test in the upper thermocline and *T. sacculifer* calcifies between these depths. The rapidly attenuating photosynthetically active radiation constrains the living depths of these symbiont-bearing species to within the upper 60 m of the euphotic zone in the southwestern Bay of Bengal. Although *G. ruber* and *N. dutertrei* calcify at different depths, as demonstrated by the different $\delta^{18}O$ values of the two species ($\Delta^{18}O_{r\text{-}d}$), large $\Delta^{18}O_{r\text{-}d}$ values were not obtained just in spring and summer when stratification is developed . The flux-weighted $\delta^{18}O$ value of a species corresponds to the mean annual $\delta^{18}O$ value of that species. Seasonal variations in species-specific test fluxes can be averaged out because of recurring flux peaks during the northeast and southwest monsoon seasons.

1 Introduction

Over the last few decades, geochemical proxies based on the chemical properties of foraminiferal tests have contributed to the elucidation of past oceanographic conditions (e.g., Liu et al., 2021; Naik et al., 2015; Nürnberg et al., 2000; Piotrowski et al., 2009; Tripati et al., 2003). Paleothermometers based on the oxygen isotope ratio ($\delta^{18}O$) (Bemis et al., 1998; Marchitto et al., 2014) and Mg/Ca ratio (Evans and Müller, 2012; Nürnberg et al., 1996) of calcareous foraminiferal tests have been widely applied. The $\delta^{18}O$ signatures of foraminifers ($\delta^{18}O_c$) mainly reflect ambient seawater temperature and $\delta^{18}O$ of seawater ($\delta^{18}O_w$), and they can be combined with independent temperature estimations obtained using the Mg/Ca thermometer in foraminifers, biomarkers, and modern satellite or in situ data to obtain salinity data (e.g., Grauel et al., 2013; Horikawa et al., 2015; Mohtadi et al., 2011; Sijinkumar et al., 2016). However, the ecological characteristics of organisms (e.g., habitat depth) and seasonal variations in production can generate errors in data obtained from single or combined proxies derived from organisms, with implications for paleoenvironmental reconstructions.

To decode the geochemical signatures of foraminiferal tests, it is essential to decipher the depth ranges over which planktic foraminifers calcify, because the chemical properties of the tests reflect the environmental conditions at those depths (Rebotim et al., 2017; Stainbank et al., 2019; Venancio et al., 2017). Although the habitat depth and calcification depth can overlap, they are different. The habitat depth of a species is the depth range at which that species dwells and concentrated populations are observed using a vertically stratified plankton tow. Planktic foraminifers exhibit species-specific habitat depths and seasonal patterns as adaptations to their optimal conditions (Jonkers and Kučera, 2017; Kretschmer et al., 2018; Rebotim et al., 2017). Moreover, the habitat depth can change as a result of descent during ontogeny and can vary at a regional scale (Jonkers and Kučera, 2017; Meilland et al., 2019; Pracht et al., 2019). The calcification depth is the depth range at which the calcite of the test is precipitated, which can be

estimated by using the geochemical signatures of tests. The calculated calcification depth range is called the apparent calcification depth (ACD), which is the mean value of ascendance during neanic stages of the life cycle and descent during gametogenesis. Discrepancies between the habitat depth (estimated from plankton tows) and the ACD (inferred from geochemical signatures) result from the unevenness of the calcification rate and timing within the life cycle of a planktic foraminifer (Blanc and Bé, 1981; Lombard et al., 2010).

Constraining the range of habitat and calcification depth of planktic foraminifers is crucial. Vertically stratified plankton tow studies provide snapshots of both types of planktic foraminiferal depth range; however, continuously tracking both depths is difficult, and basic information on the vertical distribution of planktic foraminifers is limited in many regions (Jonkers and Kučera, 2017). Sediment-trap samples are an effective alternative for reconstructing seasonal ACD variations of planktic foraminifers (Venancio et al., 2017; Wejnert et al., 2013). In addition, species-specific trends in ACD can reveal hydrological conditions in different layers of the upper water column, because each species consistently calcifies in a particular layer (Birch et al., 2013; Steph et al., 2009; Williams and Healy-Williams, 1980).

The Bay of Bengal is characterized by low salinity due to freshwater input during the summer (southwest) monsoon (SWM) and prolonged oligotrophic conditions (Kumar et al., 2002; Muraleedharan et al., 2007). The semi-annually reversing Asian monsoon wind system is the dominant factor controlling the seasonal oceanographic variations in the Bay of Bengal. The Asian monsoon system, which exerts enormous influences by means of regional physical forces, constrains plankton community structures and production (e.g., Sarma et al., 2020a; Singh et al., 2015). The planktic foraminiferal fluxes exhibit clear seasonal patterns with peaks during the SWM and winter and lowest values in spring, influenced by plankton production as species-specific food sources in the Bay of Bengal (Maeda et al., 2022). In this tropical region, in which annual sea-surface temperatures vary by less than 4°C (Locarnini et al., 2018), nutrient replenishment through eddies and river systems greatly influences size-fractionated plankton productivity and alters the optimal conditions for foraminifers. Therefore, the habitat depth and ACD of planktic foraminifers may differ from those in the open ocean. Understanding the ACD in the Bay of Bengal will be useful for producing accurate paleoceanographic reconstructions in the area using planktic foraminifers

We investigated the chemical composition of planktic foraminifers collected in sediment traps moored in the southwestern Bay of Bengal. The purpose of this study was to obtain species-specific ACD values of planktic foraminifers using $\delta^{18}O$ and Mg/Ca as temperature proxies. Previously obtained data on settling particle fluxes (Rixen et al., 2017) and datasets of planktic foraminiferal fluxes and assemblages for the same sample series (Maeda et al., 2022) were also used in this study.

2 Materials and Methods

2.1 Regional setting of the Bay of Bengal

The Bay of Bengal is affected by annual reversing monsoon winds and several mesoscale and basin-scale physical processes (Vinayachandran, 2009). During the SWM (June–September), the southwest wind speed (~10 m s^{-1}) is generally higher than the northeast wind speed of the northeast monsoon (NEM; December–February) (~6 m s^{-1}). The SWM winds provide large amounts of precipitation to central and northern India; as a result, a huge amount of freshwater is

supplied to the bay as rainfall and through large rivers such as the Ganges–Brahmaputra and Godavari (Rao and Sivakumar, 2003). The large freshwater input and excess precipitation over evaporation (~2 m yr^{-1}; Prasad, 1997) reinforces the stratification with high temperature (>28°C) in SWM seasons and forms a barrier layer, the base of the mixed layer, and the top of the thermocline (Lukas and Lindstrom, 1991; Thadathil et al., 2007). Although seasonal variability has been observed in barrier-layer thickness in the Bay of Bengal (Kumari et al., 2018), even strong SWM winds do not break the barrier layer to transport cooler thermocline water into the mixed layer (Shenoi et al., 2002). However, physical processes, including tropical cyclones (fall intermonsoon: FIM), coastal upwelling (SWM), the East India Coastal Current (spring intermonsoon: SIM), Ekman pumping (NEM), and cyclonic eddies (FIM–NEM), promote biological productivity in the euphotic zone, as does terrestrial nutrient input through river plumes (mainly in coastal regions) (Gomes et al., 2000; Kumar et al., 2002, 2007; Jyothibabu et al., 2015; Sarma et al., 2013; Vinayachandran, 2009; Vinayachandran and Mathew, 2003; Vinayachandran et al., 2005). The low light level (e.g., 417–605 μmol m^{-2} s^{-1} at the surface in the SWM; Madhu et al., 2006; Jyothibabu et al., 2018) in the Bay of Bengal restricts the size distribution of phytoplankton (Sarma et al., 2020a). The depth of the photic zone varies seasonally: 48–65 m in June (Sarma et al., 2020b); 60 m during the FIM (Kumar et al., 2007); 60–100 m in the SIM (Kumar et al., 2007); 65 ± 8 m during the SWM (Lotliker et al., 2016); and 68–82 m in July (Jyothibabu et al., 2018). In addition, less than 20% of surface photosynthetically active radiation (PAR) reaches 40 m depth in the Bay of Bengal (Sarma et al., 2020a).

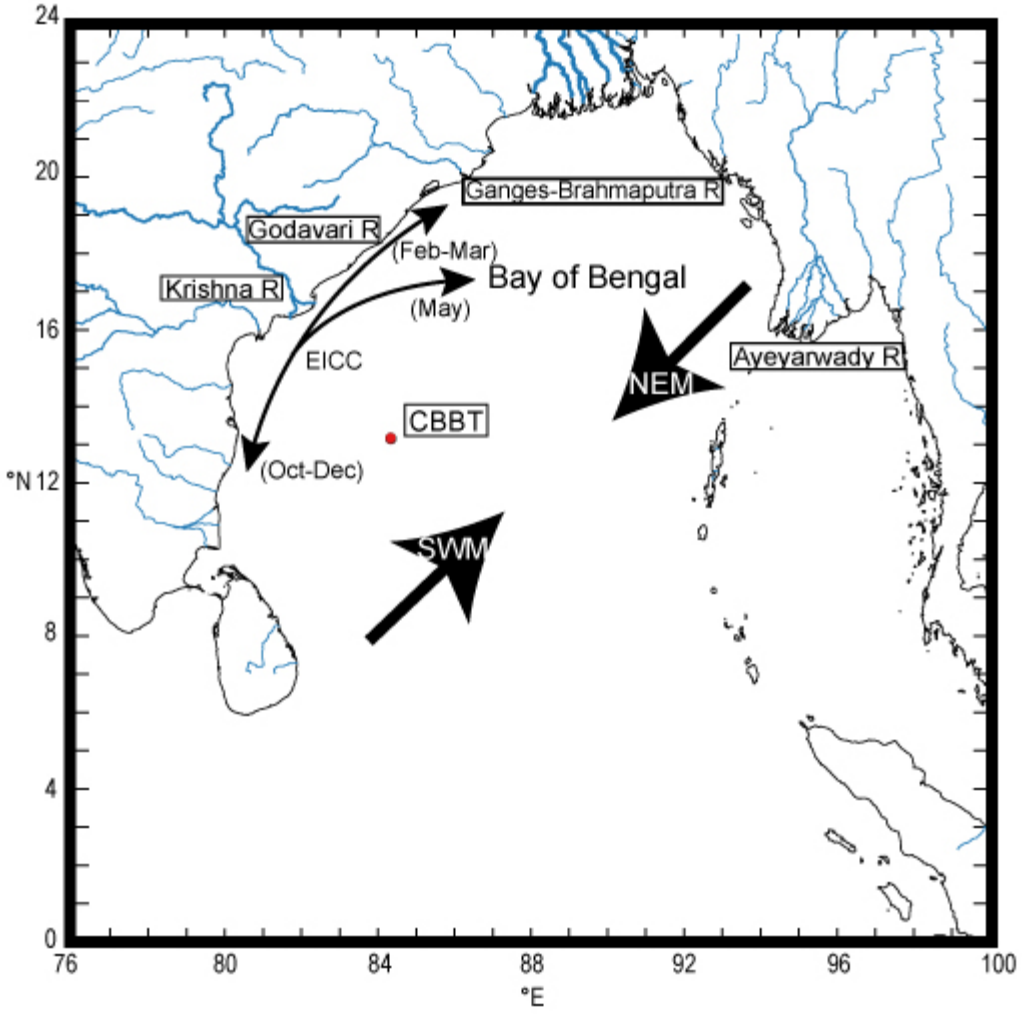

Figure 1. Map of the Bay of Bengal and the typical oceanographic settings. The red dot represents the CBBT sediment-trap mooring site in the southwestern bay, where the studied foraminifer samples were collected.The bold black arrows represent southwest monsoon (SWM) wind and northeast monsoon (NEM) wind. The black arrows representing East India Coastal Current (EICC) indicate the strong EICC in each term.

2.2 Sediment-trap sample treatments

The sediment-trap experiments were conducted as collaborative research programs between the University of Hamburg, Germany, and the National Institute of Oceanography, India. Details of the deployment and treatment of sediment traps are provided in Unger et al. (2003). PARFLUX Mark V and VI and sediment traps (Honjo and Doherty, 1988) with 0.5-m^2 collecting areas were deployed in the southwestern Bay of Bengal (Fig. 1; site CBBT). Our samples were obtained from shallow traps (862–950 m), which were labeled CBBT03 (November 1988 to October 1989), CBBT05 (December 1990 to October 1991), CBBT07 (January 1993 to October 1993), and CBBT09 (July 1995 to August 1996). The 13 (CBBT03, 05, 07) and 7 (CBBT09) time-series samples provided different 4-yr records of settling particles. The sampling intervals were 27 (CBBT03), 25 (CBBT05), 17–23 (CBBT07), and 41–42 days

(CBBT09). Prior to sediment-trap deployment, the sample cups were filled with seawater with mercuric chloride ($HgCl_2$) to hinder organic matter decomposition. After trap recovery, the samples were wet-sieved through a 1-mm nylon sieve and split into fractions using a precision rotary splitter. Then, the samples were dried at 40°C, and the samples were stored at the University of Hamburg. Planktic foraminifers were picked from the aliquots using fine brushes and sieved into four size fractions (<150, 150–250, 250–500, and 500–1000 μm). Foraminifers were identified to species level following Schiebel and Hemleben (2017) and Saito et al. (1981), as generally accepted at the time of observation. Neanic individuals and malformed specimens were not used in geochemical measurements.

We inferred that the planktic foraminifers in the sediment-trap samples were well preserved because many unbroken pteropods with thin aragonite tests were also present in the samples, the spines of glassy foraminiferal tests were preserved well; furthermore, tests of fragile species such as *Hastigerina pelagica* and *Beella* digitata were unbroken.

2.3 Measurement of isotopic signatures and trace-element concentrations

We selected three species—*Globigerinoides ruber*, *Trilobatus sacculifer*, and *Neogloboquadrina dutertrei*—for isotopic analyses and measurement of Mg/Ca ratios. Isotopic signatures were obtained from CBBT05 and CBBT09; Mg/Ca ratios were measured from CBBT03 and CBBT07. *Globigerinoides ruber* sensu stricto (*G. ruber* s.s.) and *G. ruber* sensu lato (*G. ruber* s.l.) were distinguished because the two morphospecies yielded different $\delta^{18}O$ values in a previous study (Carter et al., 2017). However, because of the limited number of specimens, Mg/Ca ratios were measured for either *G. ruber* s.s or *G. ruber* s.l. (only in CBBT07-12) in each sample. The target size ranges were 280–500 μm for *G. ruber*, 440–700 μm for *T. sacculifer*, and 460–650 μm for *N. dutertrei*. The major axes of unbroken tests were measured under a microscope because the sieve fraction method does not restrict test size sufficiently compared to measurements of individual test size (Beer et al., 2010). There was a lack of geochemical data for the SIM seasons, due to the low foraminiferal fluxes.

Prior to isotopic measurements, selected specimens were cleaned with ethanol in an ultrasonic cleaner to remove fine particles adhering to the tests. After it was confirmed that deposits had been completely removed, isotope measurements of oxygen and carbon were obtained using an isotope mass spectrometer (IsoPrime, Stockport, UK) at the Geological Survey of Japan, National Institute of Advanced Industrial Science and Technology, Tsukuba, Japan. Anhydrous phosphoric acid was added to foraminifers at 25°C and Techn2 gas was introduced to the IsoPrime. The external precision was better than ±0.1‰. The values of $\delta^{18}O$ and $\delta^{13}C$ are reported relative to the Vienna Pee Dee Belemnite (VPDB) scale using NBS-19 standards.

The cleaning protocol for Mg/Ca ratios followed the oxidative method (e.g., Barker et al., 2003). Because the sediment-trap samples were preserved well, and lacked Fe–Mn coatings, we omitted leaching with HNO_3 to avoid excessive cleaning. We partly followed the protocol of Cheng et al. (2000) for cleaning of fossil samples for trace-metal analysis, except that molar concentrations of solutions of chemical reagents were diluted twice and the period of ultrasonic cleaning was shortened owing to the fragility of the foraminiferal tests. In short, foraminiferal tests were gently crushed between glass plates and particles were removed with a fine brush. Subsequently, the samples were absorbed in methanol and MQ water in an ultrasonic bath for 15 s twice. After rinsing, organic matter was removed using an oxidizing agent (a mixture of equal amounts of 30% H_2O_2 and 0.1 M KOH, TAMAPURE AA-100 from Tama Chemicals, Ltd. and

ultrapure grade from Kanto Chemical Co. Inc., respectively) in an ultrasonic bath for 15 s. Samples were further cleaned ultrasonically in a mixture of equal parts by volume of 15% H_2O_2 and 0.5% $HClO_4$ (TAMAPURE AA-100), then repeatedly rinsed with methanol and ultrapure water. The samples were dried at 65°C, and the dried samples were dissolved in dilute ultrapure nitric acid solution (2% HNO_3) to obtain Ca concentrations of 10 μg g^{-1}. To control for instrumental drift, internal standards (Be, Sc, Y, and In) were added to HNO_3. We measured ^{24}Mg, ^{25}Mg, ^{43}Ca, and ^{44}Ca during each analysis. Mg/Ca ratios were analyzed using a Thermo Scientific iCAP-Qc inductively coupled plasma mass spectrometer (Thermo Fischer Scientific, Massachusetts, USA) at the Japan Agency for Marine-Earth Science and Technology operated in helium kinetic discrimination mode. Element counts were converted into molar ratios by an intensity ratio method based on a series of matrix-matched standard solutions. Both sample and standard solutions were prepared to ensure identical Ca concentrations of 10 μg g^{-1} (within 5%). Repeated analyses of trace elements in the standard samples (JCp-1) exhibited good agreement with the consensus Mg/Ca ratio (Hathorne et al., 2013), with a standard deviation of 0.097 and an RSD (standard deviation) value of 2.3%.

2.4 Data Collection

The Global Ocean Data Assimilation System (NCEP/GODAS, Behringer et al., 1998) dataset was downloaded through ERDDAP at the Asia-Pacific Research Data Center. Because the Bay of Bengal is generally a data-poor region compared to other parts of the Indian Ocean, vertical profiles for all the experimental periods within a 1° × 1° grid at the CBBT site were not available and there are little vertical salinity profile data. The missing CTD data were not able to be supplemented directly. Therefore, assimilated data for vertical temperature and salinity profile, GODAS, were second best way. To obtain the vertical density profile, we used the GODAS dataset of monthly vertical profiles of salinity and potential temperature within 100 km of the CBBT site. These dataset of vertical profiles were interpolated through spline polynomial function. In this study, the mixed layer depth is defined as the depth where the density (σt) is more than 0.2 kg m^{-3} greater than the surface density (Narvekar and Kumar, 2006, 2014). The top of the thermocline (isothermal layer depth) is defined as the depth at which the temperature is 1°C lower than the sea-surface temperature when the temperature profile is not inverted. If the temperature profiles exhibit inversion, the top of the thermocline is defined as the depth at which the temperatures at the top and base of the inversion layer are equal (Thadathil et al., 2007). Although the thermocline is referred to as the depth where the maximum vertical temperature gradient is displayed, in practice, regionally representative isotherms are used because of the insufficient resolution of observation instruments (Yang and Wang, 2009). According to a calculation based on buoy data from the Bay of Bengal, the 23°C isotherm is appropriate for describing the thermocline depth in the Bay of Bengal (Girishkumar et al., 2013); thus, we adopted the 23°C isotherm as the bottom of the thermocline.

The euphotic zone (EZ) is defined as the depth at which PAR has been attenuated to 1% of the level at the surface, and can be calculated as follows:

$$Ez = E0 \exp(-kPAR*z) \quad (1)$$

where Ez denotes the light intensity at depth z, E0 is the light intensity at the surface, and kPAR is the attenuation coefficient for PAR. In the present study, the mean monthly PAR profile (January 2003–June 2007) was obtained from PAR data observed by MODIS aqua within 1° × 1° grids at the CBBT site. The kPAR range in the southwestern Bay of Bengal was 0.075–0.1 m^{-1} (Lotliker et al., 2016). The calculated EZ depth ranges are illustrated in Fig. 2, and the EZ depth range was confirmed by in situ observational data from the Bay of Bengal (Jyothibabu et al., 2018; Kumar et al., 2007; Lotliker et al. 2016; Sarma et al., 2020a, b).

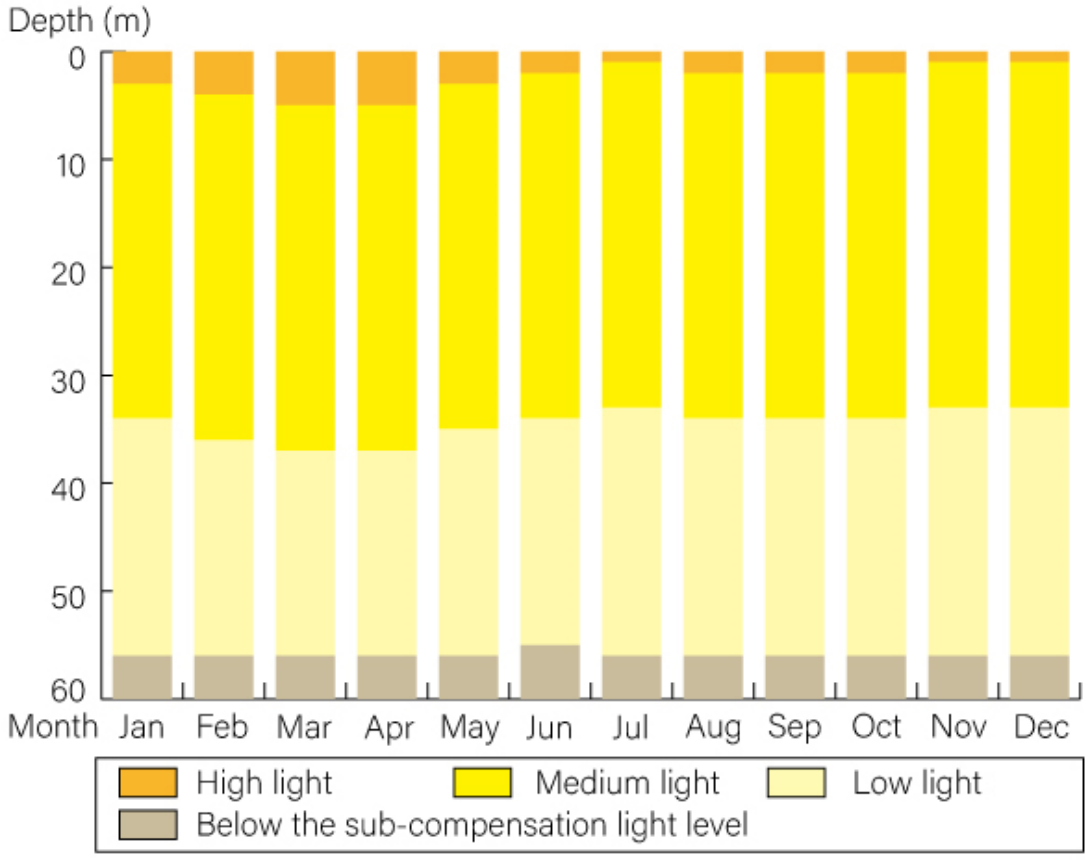

Figure 2. The monthly euphotic zone depth ranges calculated from satellite data in the southwestern Bay of Bengal. The kPAR value for calculation was 0.0875 m^{-1}, which is the average of kPAR in the southwestern Bay of Bengal (Lotliker et al., 2016). The ranges of high (>380 µmol m^{-2} s^{-1}), medium (26–380 µmol m^{-2} s^{-1}), and low light (<26 µmol m^{-2} s^{-1}) columns represent the ranges of respective light levels in Bemis et al. (1998) and sub-compensation light level (foraminiferal respiration > photosynthesis) for *Trilobatus sacculifer* (Jørgensen et al., 1985).

The $\delta^{18}O_w$–S relationships in the Bay of Bengal are complicated because of mixing of different riverine inputs with various $\delta^{18}O$ values at the regional scale; therefore, there is no uniform overall $\delta^{18}O_w$–S relationship for the Bay of Bengal (Achyuthan et al., 2013). We adopted $\delta^{18}O_w$–S relationships for each season for the central and the southwestern Bay of Bengal from Achyuthan et al. (2013) for June–October (Eq. 2), and Kumar et al. (2018) for winter (Eq. 3) and spring (Eq. 4).

262

263 $\delta^{18}O_w = 0.14S - 4.7$ (2)

264 $\delta^{18}O_w = 0.14S - 4.58$ (3)

265 $\delta^{18}O_w = 0.28S - 9.1$ (4)

266

267 Previous studies have proposed $\delta^{18}O$–temperature calibrations based on inorganic calcite
268 (Kim and O'Neil, 1997), cultured specimens (Bemis et al., 1998; Bouvier-Soumagnac and
269 Duplessy, 1985; Erez and Luz, 1983), plankton-tow studies (Mulitza et al., 2003), and surface
270 sediments (Farmer et al., 2007). Equations based on cultured specimens are preferable when
271 selecting $\delta^{18}O$–temperature equations; thus, we used equations obtained by culture studies as far
272 as possible. However, the equation for *N. dutertrei* (Bouvier-Soumagnac and Duplessy, 1985)
273 has been reported to yield lower temperatures (Wejnert et al., 2013) than actual values, and so
274 we did not use it. Equations for *Table*cultured under high light (>380 μmol m^{-2} s^{-1}) and low light
275 conditions (20–30 μmol m^{-2} s^{-1}) are appropriate to our dataset for *G. ruber*, *T. sacculifer*, and *N.*
276 *dutertrei* (Bemis et al., 1998). We followed the traditional step in foraminiferal paleotemperature
277 equations to convert $\delta^{18}O_{sw}$ on the Vienna Standard Mean Ocean Water (VSMOW) scale into the
278 VPDB scale by subtracting 0.27‰. We included this step because the scale conversion of Kim et
279 al. (2015) could not be used, because of the lack of $\delta^{18}O$ data in the study of Bemis et al. (1998).

280 Mg/Ca–temperature equations have been proposed in several studies (e.g., Anand et al.,
281 2003; Gray et al., 2018) using both multi-species calibrations and species-specific calibrations.
282 We selected the Mg/Ca–temperature equation for *G. ruber* proposed in Gray et al. (2018),
283 because this equation is based on sediment-trap/plankton-tow samples including CBBT samples
284 (CBBT06). Although Gray et al. (2018) included the influence of pH or [CO_3^{2-}], carbonate
285 system data in the Bay of Bengal are sparse and some data were collected in the coastal region
286 that is influenced by riverine input (Land et al., 2019). Thus, we adopted the Mg/Ca–temperature
287 equation without a carbonate system term (Gray et al., 2018). For *T. sacculifer* and *N. dutertrei*,
288 the equations proposed by Anand et al. (2003) for spinose and non-spinose species, respectively,
289 were used because the equations were obtained using sediment-trap samples.

290 **3 Results**

291 3.1 Foraminiferal Assemblage of CBBT09

292 The foraminiferal assemblages in CBBT09 are described in Fig. 3. The fluxes of planktic
293 foraminifers varied between 52 and 1093 individuals m^{-2} d^{-1}. The highest values occurred in the
294 NEM season, the fluxes were lower in the SWM season, and the lowest flux was in spring. The
295 dominant species were *G. ruber*, *T. sacculifer*, *Globigerinella siphonifera*, *N. dutertrei*,
296 *Globigerinita glutinata*, *Globigerina bulloides*, and *Globorotalia menardii*, consistent with
297 CBBT samples from other sampling periods (see Figs. 3–5 in Maeda et al., 2022). The fluxes of
298 *G. glutinata*, *G. bulloides*, *G. siphonifera*, *N. dutertrei*, and *G. ruber* were higher in the NEM
299 season than in SWM periods. The fluxes of *G. menardii* and *T. sacculifer* were bimodal, with
300 comparable fluxes during the SWM and NEM periods.

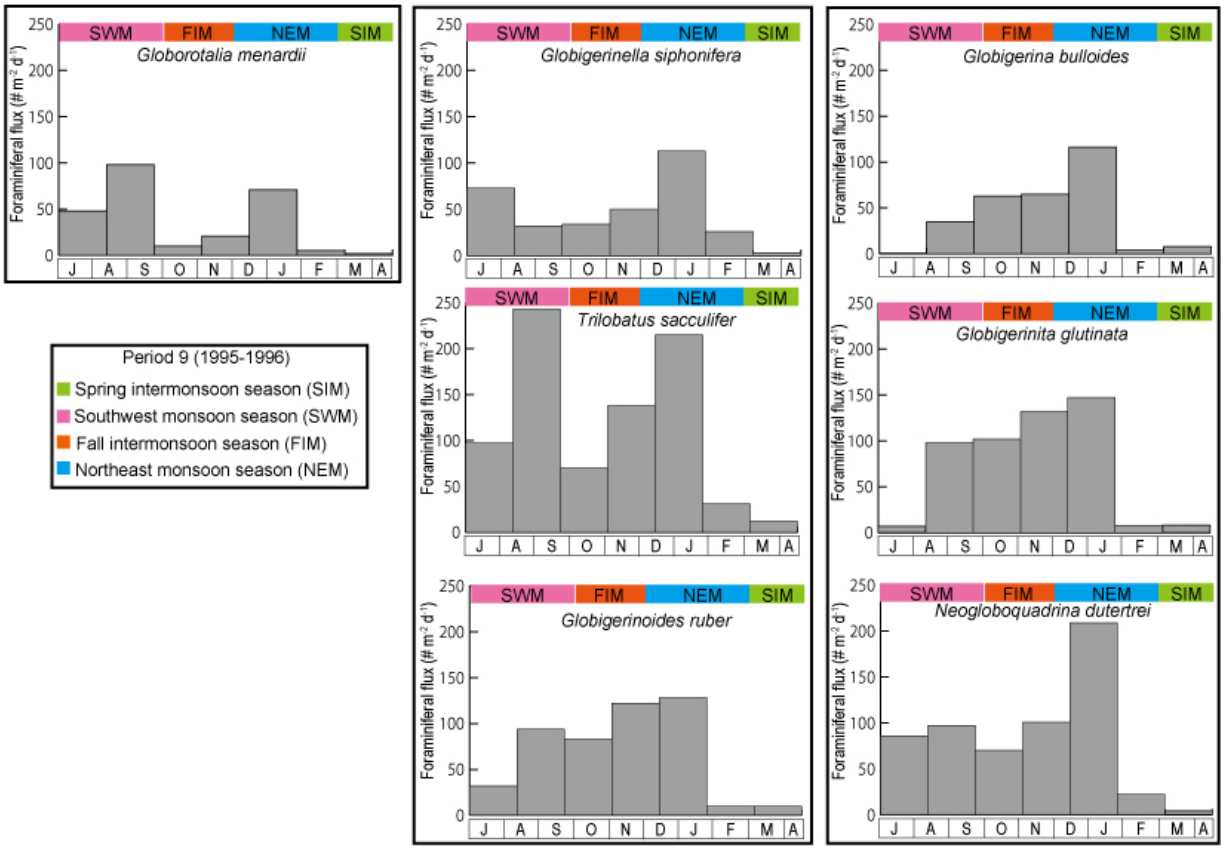

Figure 3. The result of planktic foraminiferal fluxes and assemblages for dominant seven species in CBBT09.

3.2 Oxygen and carbon isotope ratios

The $\delta^{18}O$ and $\delta^{13}C$ results for *G. ruber*, *T. sacculifer*, and *N. dutertrei* are provided in Fig. 4. The $\delta^{18}O$ ranges were different for each species. The $\delta^{18}O$ values of *G. ruber* s.l. varied between −3.36‰ and −2.71‰, and those of *G. ruber* s.s. were −3.32‰ to −2.48‰. In most samples, the $\delta^{18}O$ values of both morphotypes of *G. ruber* were within two standard deviations. The $\delta^{18}O$ values of *T. sacculifer* and *N. dutertrei* were heavier than those of *G. ruber*, ranging from −2.82‰ to −1.96‰ and −2.68‰ to −1.78‰, respectively. The $\delta^{18}O$ of *G. ruber* was lightest during SWM seasons in both CBBT05 and CBBT09. In contrast, the $\delta^{18}O$ values of *T. sacculifer* gradually decreased from the FIM to NEM seasons, with markedly low values in January–February. The seasonality of $\delta^{18}O$ values in *N. dutertrei* differed from those of the other species, with peaks in May (CBBT05) and July–August (CBBT09) and lower values in NEM seasons. The $\delta^{13}C$ values of *G. ruber* s.s. and *G. ruber* s.l. were 0.59‰–1.18‰ and 0.60‰–0.88‰, respectively. *Trilobatus sacculifer* and *N. dutertrei* exhibited wider $\delta^{13}C$ ranges of 0.49‰–1.27‰ and 0.63‰–1.66‰, respectively.

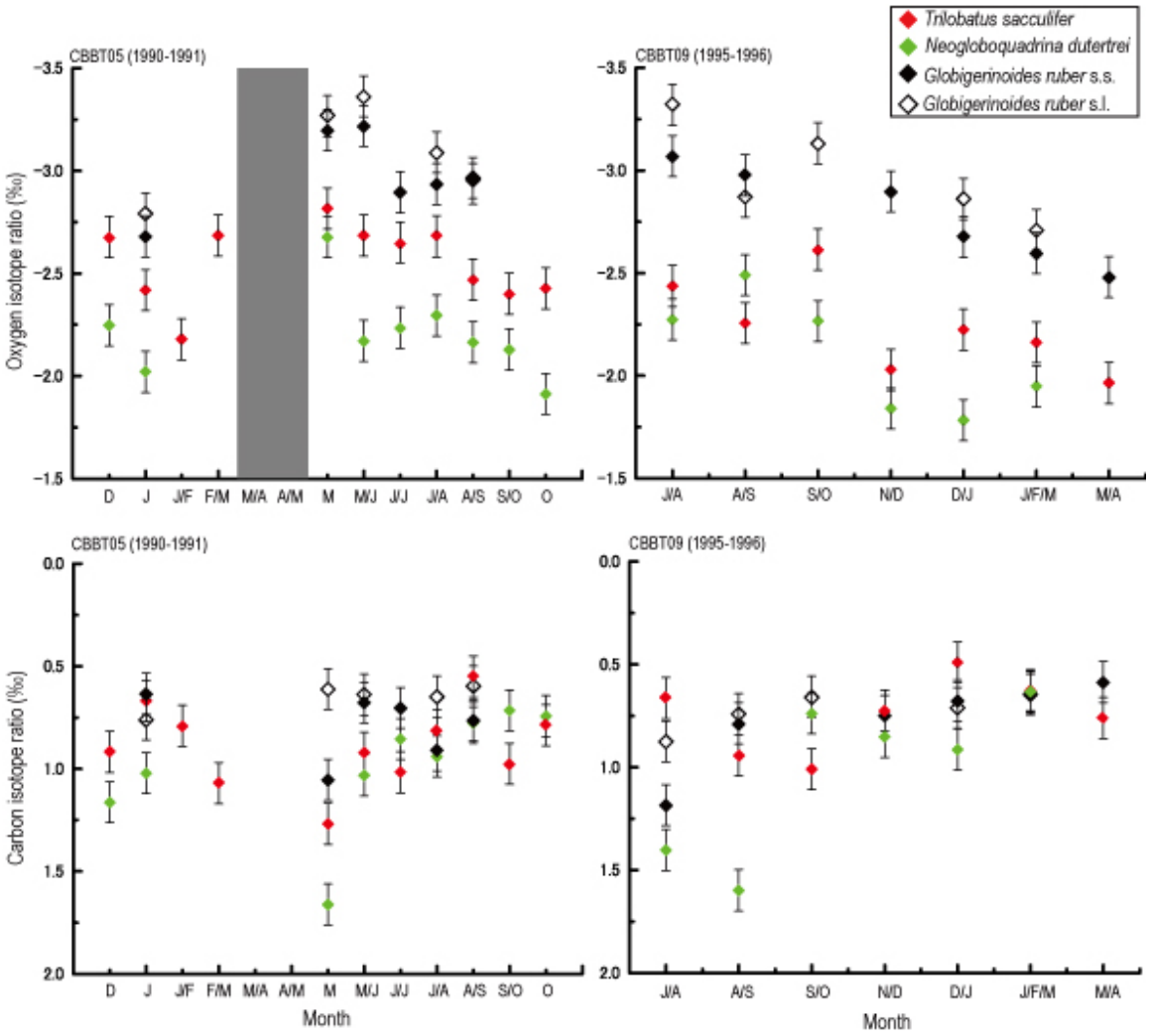

Figure 4. The results of oxygen (upper panels) and carbon isotope ratios (lower panels). Green rhombi mean *Neogloboquadrina dutertrei*, red ones mean *Trilobatus sacculifer* and black ones represent *Globigerinoides ruber*. The gray shades in CBBT05 represent the lack of data.

3.3 Mg/Ca ratios

The Mg/Ca ratios of *G. ruber* were 5.41–7.04 mmol mol^{-1} and those of *T. sacculifer* were 3.75–4.95 mmol mol^{-1} (Fig. 5). The Mg/Ca range of *N. dutertrei* was lower, 2.85–4.61 mmol mol^{-1}.

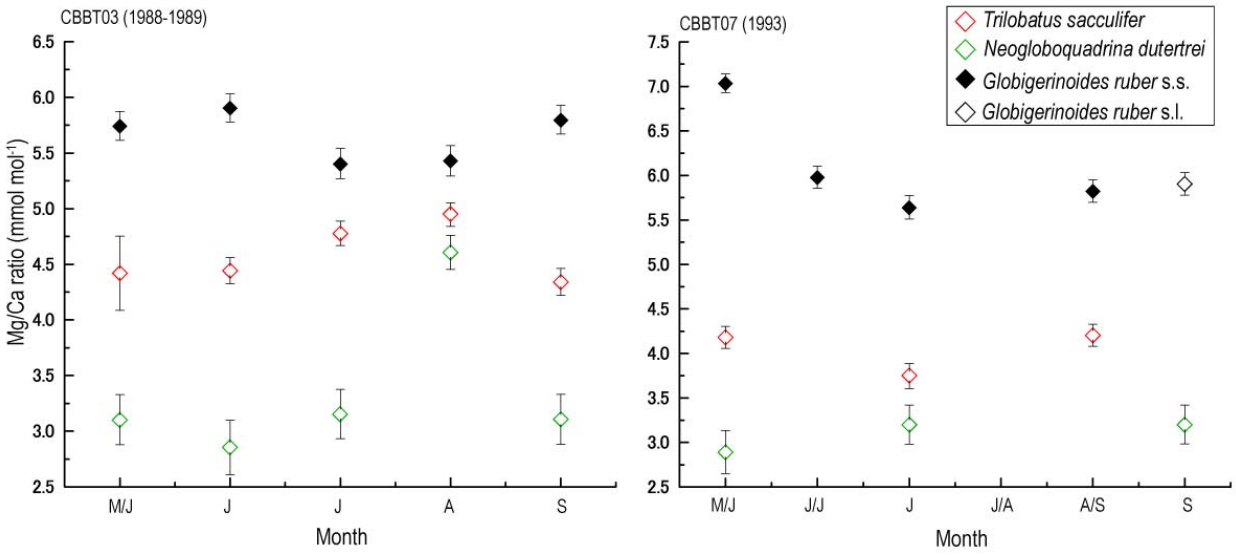

Figure 5. The Mg/Ca ratios in CBBT03 (left) and CBBT07 (right). Green rhombi mean *Neogloboquadrina dutertrei*, red ones mean *Trilobatus sacculifer* and black ones represent *Globigerinoides ruber*.

4 Discussion

4.1 Species-specific temperature records calibrated from signatures and calcification depths

The temperatures calculated from the $\delta^{18}O$ data for each species are listed in Table S5. The $\delta^{18}O$–temperature calibrations obtained from cultured *O. universa* (Bemis et al., 1998) were applied to infer the temperature records for each species. Summaries of the water-column structure based on the GODAS dataset with ACD ranges for each species during the four observational periods are provided in Fig. 6.

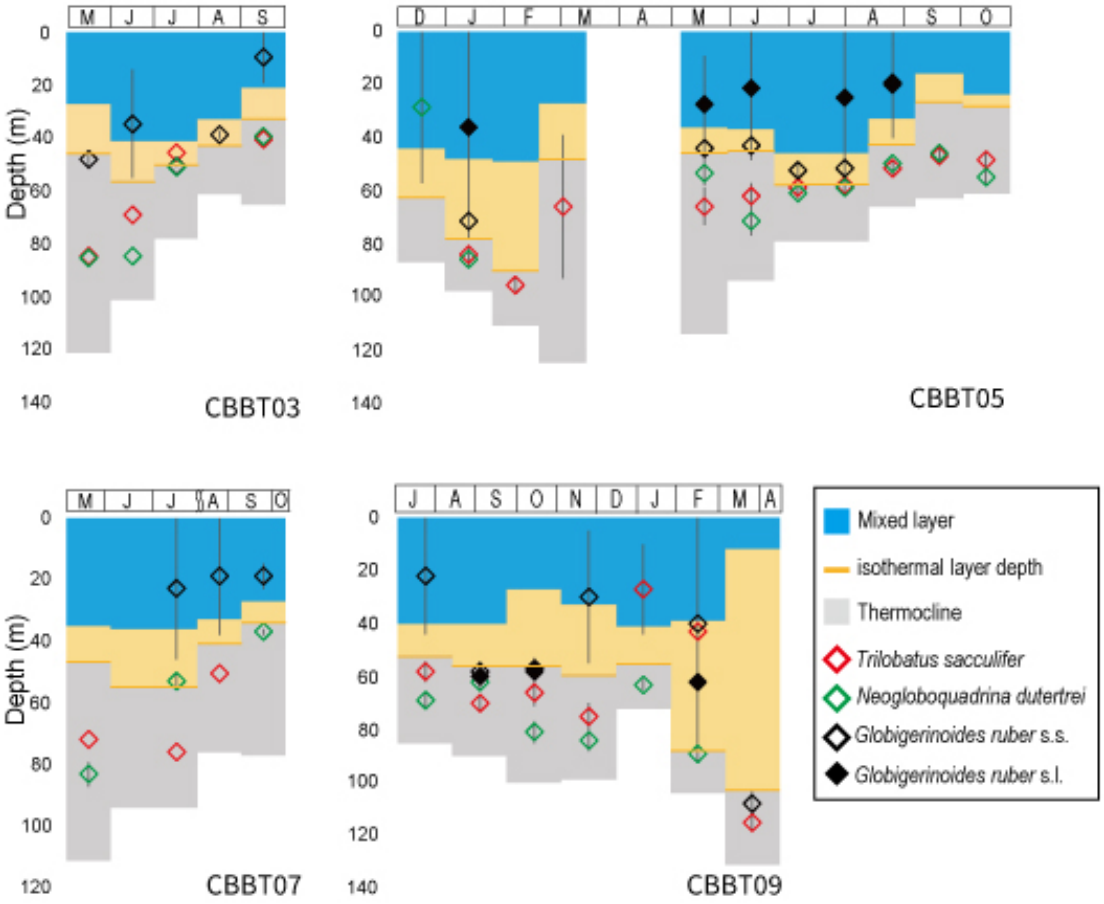

Figure 6. The water column structure (blue: mixed layer, yellow: between the mixed layer and thermocline, gray: thermocline) with apparent calcification depth ranges for three planktic foraminifers in CBBT03 (upper left), CBBT05 (upper right), CBBT07 (lower left), and CBBT09 (lower right). The x-axis represent month.

4.1.1 *Globigerinoides ruber*

The $\delta^{18}O$–temperature ranges of *G. ruber* s.s. and *G. ruber* s.l. were 26.2–29.1°C and 26.8–29.5°C, respectively, in CBBT05, and 26.1–28.4°C and 26.9–29.6°C, respectively, in CBBT09. The SWM temperature was 27.5–29.1°C in CBBT03 and 28.3–32.5°C in CBBT07. Both morphotypes of *G. ruber* showed comparable $\delta^{18}O$–temperature ranges in each sample.

The $\delta^{18}O$– and Mg/Ca–temperature patterns of *G. ruber* are primarily consistent with the mixed-layer temperature records of the Bay of Bengal in all sample series (Fig. 6). The ACD ranges for *G. ruber* were 0–51 m in CBBT03, 0–78 m in CBBT05, 0–41 m in CBBT07, and 0–113 m in CBBT09. The symbiont-bearing species *G. ruber* is considered to inhabit the EZ. Because the monthly EZ in the Bay of Bengal reaches ~60 m, *G. ruber* dwells in the upper 60 m. Moreover, *T. sacculifer* exhibited a functional absorption cross-section of photosystem II (σPSII) comparable to that of *G. ruber* (white) (Takagi et al., 2019), suggesting that *G. ruber* requires a sub-compensation light level (i.e., foraminiferal respiration > photosynthesis) similar to that of *T. sacculifer* (26–30 μmol m^{-2} s^{-1}; Jørgensen et al., 1985). Even if the fertile states in seawater affect the growth of *G. ruber*, in culture experiments with a light level of 50–60 μmol m^{-2} s^{-1},

this species achieved sizes of more than 400 μm (Bijma et al., 1992). Light levels of 26–30 μmol m^{-2} s^{-1} occur at 35–40 m depth in the Bay of Bengal. The depth ranges of the mixed layer were 15–55 m, including the part of the EZ with a sufficient light intensity for *G. ruber*, consistent with the estimated ACD range of this species. In summary, accurate reconstructions of ACD were hindered by the lack of in situ CTD data and complicated $\delta^{18}O_w$ mixing in the Bay of Bengal; however, the light conditions suggest that *G. ruber* calcifies within the mixed layer. Mixed layer calcification of *G. ruber* is consistent with previous studies reporting that the $\delta^{18}O$–temperature relationship of *G. ruber* reflects the mixed layer temperature, because *G. ruber* occurs in the surface mixed layer (Duplessy et al., 1981; Stoll et al., 2007), as has been demonstrated for concentrated populations in multi-plankton net studies (Peeters and Brummer, 2002).

4.1.2 *Neogloboquadrina dutertrei*

The calculated temperature ranges for *N. dutertrei* were lower than those of *G. ruber*. The temperature range was 25.6–34.2°C in CBBT03, 23.8–28.2°C in CBBT05, 25.8–27.7°C in CBBT07, and 24.5–27.2°C in CBBT09. The $\delta^{18}O$ values of *N. dutertrei* were heavier than those of *G. ruber*, and yielded ACD estimates of 59–81 m in CBBT03, 0–90 m in CBBT05, 44–93 m in CBBT05, and 47–92 m in CBBT09. The most frequent ACD range was 50–75 m, consistent with the thermocline depth in the Bay of Bengal. *Neogloboquadrina dutertrei* is a symbiont-facultative species (pelagophyte-symbiont; Bird et al., 2018), and previous field observations have reported that up to 94% of individuals possess functional chlorophyll a (chl-a ; Takagi et al., 2019). The dominance of symbiont-facultative individuals suggests that *N. dutertrei* can dwell in the EZ, and the higher σPSII of this species implies that it is adapted to a low light level (Takagi et al., 2019). *Neogloboquadrina dutertrei* has been observed to prefer an herbivorous diet, but a recent study reported that the species assimilates substantial amounts of protists from particulate organic matter (Bird et al., 2018). The development of the subsurface microbial loop with the subsurface chl-a maximum (>60 m) in spring and the high flux of *N. dutertrei* in May and June in the southwestern Bay of Bengal are consistent with the hypothesis that *N. dutertrei* inhabits the thermocline and is reliant on subsurface primary production and remineralized organic carbon (Kumar et al., 2007; Subha Anand et al., 2017). Experiments on laboratory cultures of *N. dutertrei* under diurnal light/dark cycles have indicated that this species tends to precipitate its entire test as a thin calcite layer, then thickens the test by adding an outer calcite layer with Mg-banding (Fehrenbacher et al., 2017). Thus, the ACD may reflect the living depth in the final stage of the life cycle for *N. dutertrei*. The heavier $\delta^{13}C$ ranges of *N. dutertrei* than of *G. ruber* and *T. sacculifer* agree with the results from plankton net samples (Fairbanks et al., 1982), which suggest that the habitat depth of *N. dutertrei* can overlap the habitat depth ranges of *G. ruber* and *T. sacculifer*.

4.1.3 *Trilobatus sacculifer*

Trilobatus sacculifer exhibited a temperature range of 26.8–28.6°C in CBBT03, 25.1–27.6°C in CBBT05, 24.9–26.4°C in CBBT07, and 23.9–26.0°C in CBBT09. The ACD ranges were 0–82 m in CBBT03, 0–81 m in CBBT05, 69–85 m in CBBT07, and 35–93 m in CBBT09. The species descends later in its ontogeny with the formation of a sac-like chamber and gametogenic calcite (Bé, 1980; Takagi et al., 2015); in this study, *T. sacculifer* without sacs exhibited substantially heavier $\delta^{18}O$ values and deeper ACD ranges than those of *G. ruber*. Because *T. sacculifer* possesses dinoflagellates as symbiont algae and symbiotic photosynthesis

helps to regulate host calcification (Bé et al., 1982; Caron et al., 1982), we infer that this species also calcifies within the EZ. An early culture study indicated that the sub-compensation light level for the species is 26–30 μmol m^{-2} s^{-1} (Jørgensen et al., 1985): this light level occurs at 35–40 m depth in the southwestern Bay of Bengal. In addition, Lombard et al. (2010) reported that *T. sacculifer* calcified 30% less under 35 μmol m^{-2} s^{-1} than under 335 μmol m^{-2} s^{-1} and the σPSII values of dinoflagellate-symbiont species indicate a high-light-adapted photophysiology (Jørgensen et al., 1985; Spero and Parker, 1985; Takagi et al., 2019). Under higher light levels, *T. sacculifer* forms heavier and larger tests and individuals need a light level greater than 8–10 μmol m^{-2} s^{-1} to grow up to 500–600 μm in size: PAR is attenuated to that level at 50 m in the southwestern Bay of Bengal (Spero and Lea, 1993). Therefore, the estimated ACD of *T. sacculifer* may be deeper than the actual habitat depth in the EZ (<60 m). The discrepancy between the ACD and the EZ is attributed to the sparse dataset, limited equations for calibration, and vital effects such as rapid addition of gametogenic calcite with 1.0‰–1.4‰ heavier $\delta^{18}O$ in the last stage of the lifecycle (Blanc and Bé, 1981; Wycech et al., 2018). Therefore, *T. sacculifer* can apparently reflect the temperature between the lower mixed layer and upper thermocline, although this species may calcify in the lower mixed layer.

4.2 Implications for paleoceanographic reconstruction

Vertical hydrological gradients have been reconstructed using species-specific depth habitats of planktic foraminifers; for example, the $\delta^{18}O$ difference between *T. sacculifer* and *G. truncatulinoides* or *G. ruber* and *N. dutertrei* ($\Delta^{18}O_{r\text{-}d}$) has been applied as an indicator of the strength of stratification (Mulitza et al., 1997; Nilsson-Kerr et al., 2022; Ota et al., 2019). The energy required for mixing (ERM) of water column indicates the difference between the potential energy of a stratified and unstratified column in a certain depth (Shenoi et al., 2002), which often used to evaluate water column stratification. According to Fousiya et al. (2016), Monthly ERM within the EZ (50 m depth) calculated from GODAS in the Bay of Bengal reaches the maxima in the FIM and the minima in the NEM. Although ERM values using GODAS are often underestimated compared to ERM with observation data (Fousiya et al., 2016), the consistent trends exhibit. $\Delta^{18}O_{r\text{-}d}$ peaks occurred prior to the SWM in CBBT05, but during the NEM in CBBT09 (Fig. 7). Thus, the $\Delta^{18}O_{r\text{-}d}$ signatures do not reflect the ERM trends.

The $\Delta^{18}O_{r\text{-}d}$ as a stratification proxy requires an assumption that both target species habit in the same depth range; mixed layer and thermocline. However, the $\delta^{18}O$ signatures of *G. ruber* did not always indicate within the mixed layer, which decreased the $\Delta^{18}O_{r\text{-}d}$ (Fig. 6). Furthermore, oligotrophic condition leading a short effective food web in the Bay of Bengal (Jyothibabu et al., 2008; Fernandes and Ramaiah, 2014; Arunpandi et al., 2022) provide large variations in standing stocks and timing of increase for planktic foraminifers (Maeda et al., 2022). The plankton production including planktic foraminifers is strongly influenced by sporadic mesoscale eddies in addition to seasonal monsoon winds and currents (Jyothibabu et al., 2015; Sarma et al., 2020a; Vinayachandran et al., 2009). Thus, the optimum feeding conditions for *G. ruber* and *N. dutertrei* could change vertically and temporally every year, it is hard to hold the requirements for $\Delta^{18}O_{r\text{-}d}$ in the Bay of Bengal.

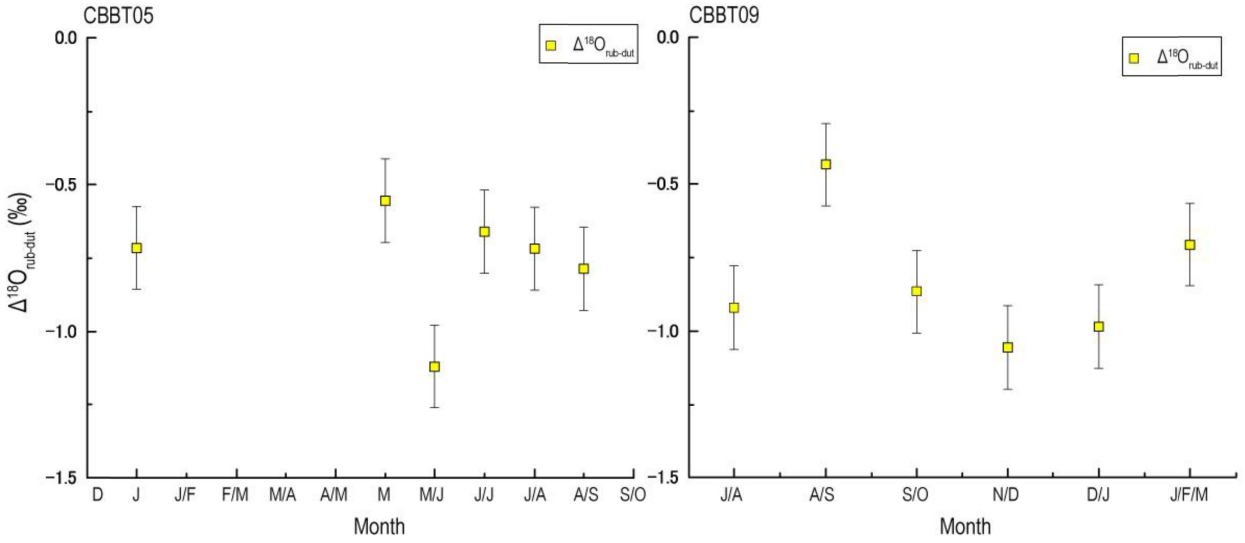

Figure 7. The difference of $\delta^{18}O$ between *Globigerinoides ruber* and *Neogloboquadrina dutertrei* ($\Delta^{18}O_{r\text{-}d}$) in CBBT05 (left) and CBBT09 (right).

Annual flux-weighted mean $\delta^{18}O$ values have been applied to understand the influence of seasonal flux patterns on $\delta^{18}O$ signatures recorded in marine sediments (e.g., Tedesco et al., 2007). The flux-weighted $\delta^{18}O$ was calculated as given in Venancio et al. (2017) based on the fundamental model of Mix (1987) and discussions in Mulitza et al. (1998) as follows:

$$\boldsymbol{\delta^{18}O_{FW}} = \sum_{i=1}^{n} \frac{(\boldsymbol{flux_i \times \delta_{ci}})}{\boldsymbol{total\ flux}} \quad (5)$$

where $\delta^{18}O_{Fw}$ represents the flux-weighted $\delta^{18}O$ value, and $flux_i$ and δc_i denote the species-specific planktic foraminiferal flux and the $\delta^{18}O$ value of tests in each sample, respectively.

Table 1. The comparison of annual mean $\delta^{18}O$ and flux weighted $\delta^{18}O$ for each species

Species	flux-weighted $\delta^{18}O$ (‰)	Annual mean $\delta^{18}O$ (‰)
Globigerinoid ruber	-2.91	-2.86
Trilobatus sacculifer	-2.55	-2.55
Neogloboquadrina dutertrei	-2.20	-2.21

Unfortunately, the low fluxes of all species in the SIM and the restricted time intervals of sample collection influenced the annual flux-weighted $\delta^{18}O$ values for each species. *Neogloboquadrina dutertrei* showed the maximum peak in May/June in all observational years. However, the limited $\delta^{18}O_r$ data prohibit accurate calculation of flux-weighted $\delta^{18}O_r$. Even though there is a lack of $\delta^{18}O$ data in March/April and April/May for *T. sacculifer*, the fluxes in both samples accounted for approximately 1.4%. Therefore, the appropriate $\delta^{18}O$ dataset for *G. ruber* was CBBT09 and for *T. sacculifer* and *N. dutertrei* were CBBT05. In calculating the flux-weighted $\delta^{18}O_r$, we adopted mean $\delta^{18}O$ values for *G. ruber* s.s. and *G. ruber* s.l. The flux-weighted $\delta^{18}O$ value for each species was −2.91‰ for *G. ruber*, −2.55‰ for *T. sacculifer*, and −2.20‰ for *N. dutertrei* (Table 1). The flux-weighted $\delta^{18}O$-temperatures for *T. sacculifer*

(28.9°C) and *N. dutertrei* (27.2°C) were apparently biased to be similar to the SIM to SWM high temperatures in the upper thermocline and the mixed layer. For *G. ruber* (27.7°C), the flux-weighted $\delta^{18}O$-temperature appears to be biased towards the Tml in the NEM. However, the mean $\delta^{18}O$ values of the three species were in good agreement with the flux-weighted $\delta^{18}O$ values (Table 1); therefore, although species-specific seasonal patterns of test fluxes were observed in CBBT sediment-trap samples, the influence of the seasonal biases in foraminiferal fluxes was averaged out because of the recurring flux peaks in the SWM and the NEM. In addition, the flux-weighted $\delta^{18}O$ value of *G. ruber* was consistent with previously obtained $\delta^{18}O_r$ values of −2.80‰ ± 0.08‰ (698 y; Da Silva et al., 2017), −2.65‰ ± 0.08‰ (1.18 ka BP; Liu et al., 2021), and −2.82‰ ± 0.1‰ (0 y; Ponton et al., 2012) from core-top samples collected in the Bay of Bengal. This finding that the measured $\delta^{18}O$ values of planktic species in sediment assemblages reflect the mean annual $\delta^{18}O$ values will provide strong support for future paleoceanographic reconstructions in the Bay of Bengal.

5 Conclusions

The $\delta^{18}O$ and Mg/Ca signatures of planktic foraminifers in sediment-trap samples collected from the southwestern Bay of Bengal were investigated to reveal the ACD for each species.

1. The temperature ranges estimated from $\delta^{18}O$ and Mg/Ca data indicated species-specific ACDs: *G. ruber* in the mixed layer; *T. sacculifer* between the lower mixed layer and the upper thermocline; and *N. dutertrei* in the upper thermocline.

2. The low light level in the Bay of Bengal strongly constrains the ACD of each species. The ACDs of *G. ruber* and *N. dutertrei* are consistent with the light conditions and their photosynthetic strategies. The ACD range of *T. sacculifer* was biased, being apparently too deep for sufficient growth, because of the higher $\delta^{18}O$ values of gametogenic calcite.

3. $\Delta^{18}O_{r\text{-}d}$ may not be appropriate as a proxy of surface stratification in the Bay of Bengal. However, the flux-weighted $\delta^{18}O$ of each species was consistent with the mean $\delta^{18}O$ values, and the interannual variation in seasonal trends in fluxes and assemblages of planktic foraminifers can be averaged out.

Acknowledgments

We appreciate the great contribution to isotope measurements made by Ms. Y. Yoshinaga of AIST. We thank Ms. Y. Yoshikawa of JAMSTEC for assistance with the trace-element analysis. We thank the technicians, officers, and crews of the research expeditions on ORV *Sagar Kanya* and R/V *Sonne* for their support on board. This work was supported by Grant-in-Aid for JSPS Fellows [grant number JP18J21600].

Open Research

The foraminiferal fluxes of sediment-trap materials in CBBT03, 05, and 07 are available in the paper and its supporting information of Maeda et al. (2022) and in PANGAEA Data Publisher for Earth & Environmental Science at Rixen et al. (2017). The dataset for The foraminiferal fluxes of in CBBT09

and chemical property of foraminifers will be available at Zenodo. GODAS dataset (Behringer et al., 1998, https://psl.noaa.gov/data/gridded/data.godas.html) can be available through ERDDAP at the Asia-Pacific Research Data Center (http://apdrc.soest.hawaii.edu/index.php). Monthly PAR profile dataset can be available in MODIS aqua (https://oceancolor.gsfc.nasa.gov/data/aqua/).

References

Achyuthan, H., Deshpande, R. D., Rao, M. S., Kumar, B., Nallathambi, T., Kumar, K. S., Rameshe, R., Ramachandrane, P., Maurya, A.S., & Gupta, S. K. (2013). Stable isotopes and salinity in the surface waters of the Bay of Bengal: implications for water dynamics and palaeoclimate. *Marine Chemistry*, 149, 51-62. https://doi.org/10.1016/j.marchem.2012.12.006

Anand, P., Elderfield, H., & Conte, M. H. (2003). Calibration of Mg/Ca thermometry in planktonic foraminifera from a sediment trap time series. *Paleoceanography*, 18(2). https://doi.org/10.1029/2002PA000846

Arunpandi, N., Jyothibabu, R., Jagadeesan, L., Lekshmi, S., Surya, S., & Biju, A. (2022). Copepod carcasses in the western Bay of Bengal and associated ecology. *Environmental Monitoring and Assessment*, 194(2). https://doi.org/10.1007/s10661-021-09748-x

Barker, S., Higgins, J. A., & Elderfield, H. (2003). The future of the carbon cycle: review, calcification response, ballast and feedback on atmospheric CO2. *Philosophical Transactions of the Royal Society of London. Series A: Mathematical, Physical and Engineering Sciences*, 361(1810), 1977-1999. https://doi.org/10.1098/rsta.2003.1238

Bé, A. W. H. (1980). Gametogenic calcification in a spinose planktonic foraminifer, *Globigerinoides sacculifer* (Brady). *Marine Micropaleontology*, 5, 283-310. https://doi.org/10.1016/0377-8398(80)90014-6

Bé, A. W. H., Spero, H. J., & Anderson, O. R. (1982). Effects of symbiont elimination and reinfection on the life processes of the planktonic foraminifer *Globigerinoides sacculifer*. *Marine Biology,* 70(1), 73-86. https://doi.org/10.1007/BF00397298

Beer, C. J., Schiebel, R., & Wilson, P. A. (2010). On methodologies for determining the size-normalised weight of planktic foraminifera. *Biogeosciences*, 7(7), 2193-2198. https://doi.org/10.5194/bg-7-2193-2010

Bemis, B. E., Spero, H. J., Bijma, J., & Lea, D. W. (1998). Reevaluation of the oxygen isotopic composition of planktonic foraminifera: Experimental results and revised paleotemperature equations. *Paleoceanography*, 13(2), 150-160. https://doi.org/10.1029/98PA00070

Behringer, D.W., Ji, M., & Leetmaa, A. (1998). An improved coupled model for ENSO prediction and implications for ocean initialization. Part I: The ocean data assimilation system. Mon. Wea. Rev., 126, 1013-1021.

Bijma, J., Hemleben, C., Oberhaensli, H., & Spindler, M. (1992). The effects of increased water fertility on tropical spinose planktonic foraminifers in laboratory cultures. *The Journal of Foraminiferal Research*, 22(3), 242-256. https://doi.org/10.2113/gsjfr.22.3.242

Birch, H., Coxall, H. K., Pearson, P. N., Kroon, D., & O'Regan, M. (2013). Planktonic foraminifera stable isotopes and water column structure: Disentangling ecological signals. *Marine Micropaleontology*, 101, 127-145. https://doi.org/10.1016/j.marmicro.2013.02.002

Bird, C., Darling, K. F., Russell, A. D., Fehrenbacher, J. S., Davis, C. V., Free, A., & Ngwenya, B. T. (2018). 16S rRNA gene metabarcoding and TEM reveals different ecological strategies within the genus Neogloboquadrina (planktonic foraminifer). *PloS one*, 13(1), e0191653. https://doi.org/10.1371/journal.pone.0191653

Blanc, P. L., & Bé, A. W. (1981). Oxygen-18 enrichment of planktonic foraminifera due to gametogenic calcification below the euphotic zone. *Science*, 213(4513), 1247-1250. DOI: 10.1126/science.213.4513.1247

Bouvier-Soumagnac, Y., & Duplessy, J. C. (1985). Carbon and oxygen isotopic composition of planktonic foraminifera from laboratory culture, plankton tows and Recent sediment; implications for the reconstruction of paleoclimatic conditions and of the global carbon cycle. *The Journal of Foraminiferal Research*, 15(4), 302-320. https://doi.org/10.2113/gsjfr.15.4.302

Caron, D. A., Bé, A. W., & Anderson, O. R. (1982). Effects of variations in light intensity on life processes of the planktonic foraminifer *Globigerinoides sacculifer* in laboratory culture. *Journal of the marine biological association of the United Kingdom*, 62(2), 435-451. https://doi.org/10.1017/S0025315400057374

Carter, A., Clemens, S., Kubota, Y., Holbourn, A., & Martin, A. (2017). Differing oxygen isotopic signals of two Globigerinoides ruber (white) morphotypes in the East China Sea: Implications for paleoenvironmental reconstructions. *Marine Micropaleontology*, 131, 1-9. https://doi.org/10.1016/j.marmicro.2017.01.001

Cheng, H., Adkins, J., Edwards, R. L., & Boyle, E. A. (2000). U-Th dating of deep-sea corals. *Geochimica et Cosmochimica Acta*, 64(14), 2401-2416. https://doi.org/10.1016/S0016-7037(99)00422-6

Da Silva, R., Mazumdar, A., Mapder, T., Peketi, A., Joshi, R. K., Shaji, A., Mahalakshmi, P., Sawant, B., Naik, B. G., Carvalho, M. A., & Molletti, S. K. (2017). Salinity stratification controlled productivity variation over 300 ky in the Bay of Bengal. *Scientific reports*, 7(1), 1-7. https://doi.org/10.1038/s41598-017-14781-3

Duplessy, J. C., Bé, A. W. H., & Blanc, P. L. (1981). Oxygen and carbon isotopic composition and biogeographic distribution of planktonic foraminifera in the Indian Ocean. *Palaeogeography, Palaeoclimatology, Palaeoecology*, 33(1-3), 9-46. https://doi.org/10.1016/0031-0182(81)90031-6

Erez, J., & Luz, B. (1983). Experimental paleotemperature equation for planktonic foraminifera. *Geochimica et Cosmochimica Acta*, 47(6), 1025-1031. https://doi.org/10.1016/0016-7037(83)90232-6

Evans, D., & Müller, W. (2012). Deep time foraminifera Mg/Ca paleothermometry: Nonlinear correction for secular change in seawater Mg/Ca. *Paleoceanography,* 27(4). https://doi.org/10.1029/2012PA002315

Fairbanks, R. G., Sverdlove, M., Free, R., Wiebe, P. H., & Bé, A. W. (1982). Vertical distribution and isotopic fractionation of living planktonic foraminifera from the Panama Basin. *Nature*, 298(5877), 841-844. https://doi.org/10.1038/298841a0

Farmer, E. C., Kaplan, A., de Menocal, P. B., & Lynch - Stieglitz, J. (2007). Corroborating ecological depth preferences of planktonic foraminifera in the tropical Atlantic with the stable oxygen isotope ratios of core top specimens. *Paleoceanography,* 22(3). https://doi.org/10.1029/2006PA001361

Fehrenbacher, J. S., Russell, A. D., Davis, C. V., Gagnon, A. C., Spero, H. J., Cliff, J. B., Zhu, Z., & Martin, P. (2017). Link between light-triggered Mg-banding and chamber formation in the planktic foraminifera *Neogloboquadrina dutertrei*. *Nature communications*, 8(1), 1-10. https://doi.org/10.1038/ncomms15441

Fernandes, V., & Ramaiah, N. (2014). Distributional characteristics of surface-layer mesozooplankton in the Bay of Bengal during the 2005 winter monsoon. *Indian Journal of Geo-Marine Sciences*, Vol. 43(02).

Fousiya, T. S., Parekh, A., & Gnanaseelan, C. (2016). Interannual variability of upper ocean stratification in Bay of Bengal: Observational and modeling aspects. *Theoretical and Applied Climatology*, 126(1), 285-301. https://doi.org/10.1007/s00704-015-1574-z

Girishkumar, M. S., Ravichandran, M., & Han, W. (2013). Observed intraseasonal thermocline variability in the Bay of Bengal. *Journal of Geophysical Research: Oceans*, 118(7), 3336-3349. https://doi.org/10.1002/jgrc.20245

Gomes, H. R., Goes, J. I., & Saino, T. (2000). Influence of physical processes and freshwater discharge on the seasonality of phytoplankton regime in the Bay of Bengal. *Continental Shelf Research* 20, no. 3: 313-330. https://doi.org/10.1016/S0278-4343(99)00072-2

Grauel, A. L., Leider, A., Goudeau, M. L. S., Müller, I. A., Bernasconi, S. M., Hinrichs, K. U., de Langed, G. J., Zonneveld, K. A.F., & Versteegh, G. J. (2013). What do SST proxies really tell us? A high-resolution multiproxy ($UK'37$, $TEX^{H}86$ and foraminifera $\delta^{18}O$) study in the Gulf of Taranto, central Mediterranean Sea. *Quaternary Science Reviews*, 73, 115-131. https://doi.org/10.1016/j.quascirev.2013.05.007

Gray, W. R., Weldeab, S., Lea, D. W., Rosenthal, Y., Gruber, N., Donner, B., & Fischer, G. (2018). The effects of temperature, salinity, and the carbonate system on Mg/Ca in *Globigerinoides ruber* (white): A global sediment trap calibration. *Earth and Planetary Science Letters*, 482, 607-620. 161 https://doi.org/10.1016/j.epsl.2017.11.026

Hathorne, E. C., Gagnon, A., Felis, T., Adkins, J., Asami, R., Boer, W., Caillon, N., Case, D., Cobb, K. M., Douville, E., deMenocal, P., Eisenhauer, A., Garbe-Schönberg,D., Geibert, W., Goldstein, S., Hughen, K., Inoue, M., Kawahata, H., Kölling, M., Cornec, F. L., Linsley, B. K., McGregor, H. V., Montagna, P., Nurhati, I. S., Quinn,T. M., Raddatz, J., Rebaubier, H., Robinson, L., Sadekov, A., Sherrell, R., Sinclair, D., Tudhope, A. W., Wei, G., Wong, H., Wu, H. C., You, C.F. (2013). Interlaboratory study for coral Sr/Ca

and other element/Ca ratio measurements. *Geochemistry, Geophysics, Geosystems*, 14(9), 3730-3750. https://doi.org/10.1002/ggge.20230

Horikawa, K., Kodaira, T., Zhang, J., & Murayama, M. (2015). δ^{18}Osw estimate for *Globigerinoides ruber* from core-top sediments in the East China Sea. *Progress in Earth and Planetary Science*, 2(1), 1-20. https://doi.org/10.1186/s40645-015-0048-3

Honjo, S., & Doherty, K. W. (1988). Large aperture time-series sediment traps; design objectives, construction and application. *Deep Sea Research Part A. Oceanographic Research Papers*, 35(1), 133-149. https://doi.org/10.1016/0198-0149(88)90062-3

Jonkers, L., & Kučera, M. (2017). Quantifying the effect of seasonal and vertical habitat tracking on planktonic foraminifera proxies. *Climate of the Past,* 13(6), 573-586. https://doi.org/10.5194/cp-13-573-2017

Jørgensen, B. B., Erez, J., Revsbech, P., & Cohen, Y. (1985). Symbiotic photosynthesis in a planktonic foraminiferan, *Globigerinoides sacculifer* (Brady), studied with microelectrodes. *Limnology and Oceanography,* 30(6), 1253-1267. https://doi.org/10.4319/lo.1985.30.6.1253

Jyothibabu, R., Arunpandi, N., Jagadeesan, L., Karnan, C., Lallu, K. R., & Vinayachandran, P. N. (2018). Response of phytoplankton to heavy cloud cover and turbidity in the northern Bay of Bengal. *Scientific reports*, 8(1), 1-15. https://doi.org/10.1038/s41598-018-29586-1

Jyothibabu, R., Madhu, N. V., Maheswaran, P. A., Jayalakshmy, K. V., Nair, K. K. C., & Achuthankutty, C. T. (2008). Seasonal variation of microzooplankton (20–200 μm) and its possible implications on the vertical carbon flux in the western Bay of Bengal. *Continental Shelf Research*, 28(6), 737-755. https://doi.org/10.1016/j.csr.2007.12.011

Jyothibabu, R., Vinayachandran, P. N., Madhu, N. V., Robin, R. S., Karnan, C., Jagadeesan, L., & Anjusha, A. (2015). Phytoplankton size structure in the southern Bay of Bengal modified by the Summer Monsoon Current and associated eddies: Implications on the vertical biogenic flux. *Journal of Marine Systems*, 143, 98-119. https://doi.org/10.1016/j.jmarsys.2014.10.018

Kim, S. T., Coplen, T. B., & Horita, J. (2015). Normalization of stable isotope data for carbonate minerals: Implementation of IUPAC guidelines. *Geochimica et cosmochimica acta*, 158, 276-289. https://doi.org/10.1016/j.gca.2015.02.011

Kim, S. T., & O'Neil, J. R. (1997). Equilibrium and nonequilibrium oxygen isotope effects in synthetic carbonates. *Geochimica et cosmochimica acta*, 61(16), 3461-3475. https://doi.org/10.1016/S0016-7037(97)00169-5

Kretschmer, K., Jonkers, L., Kucera, M., & Schulz, M. (2018). Modeling seasonal and vertical habitats of planktonic foraminifera on a global scale. *Biogeosciences*, 15(14), 4405-4429. https://doi.org/10.5194/bg-15-4405-2018

Kumar, S. P., Muraleedharan, P. M., Prasad, T. G., Gauns, M., Ramaiah, N., De Souza, S. N., Sardesai, S., & Madhupratap, M. (2002). Why is the Bay of Bengal less productive during summer monsoon compared to the Arabian Sea? *Geophysical Research Letters* 29, no. 24: 88-1. https://doi.org/10.1029/2002GL016013

662 Kumar, S. P., Nuncio, M., Ramaiah, N., Sardesai, S., Narvekar, J., Fernandes, V., & Paul, J. T.
663 (2007). Eddy-mediated biological productivity in the Bay of Bengal during fall and
664 spring intermonsoons. *Deep Sea Research Part I: Oceanographic Research Papers*,
665 54(9), 1619-1640. https://doi.org/10.1016/j.dsr.2007.06.002

666 Kumar, P. K., Singh, A., & Ramesh, R. (2018). Controls on $\delta^{18}O$, δD and $\delta^{18}O$-salinity
667 relationship in the northern Indian Ocean. *Marine Chemistry*, 207, 55-62.
668 https://doi.org/10.1016/j.marchem.2018.10.010

669 Kumari, A., Kumar, S. P., & Chakraborty, A. (2018). Seasonal and interannual variability in the
670 barrier layer of the Bay of Bengal. *Journal of Geophysical Research: Oceans*, 123(2),
671 1001-1015. https://doi.org/10.1002/2017JC013213

672 Land, P. E., Findlay, H. S., Shutler, J. D., Ashton, I. G., Holding, T., Grouazel, A., Girard-
673 Ardhuin,F., Reul, N., Piolle, J. F., Chapron, B., Quilfen, Y., Bellerby, R. G. J., Bhadury,
674 P., Salisbury, J., Vandemark, D., Sabia, R. (2019). Optimum satellite remote sensing of
675 the marine carbonate system using empirical algorithms in the global ocean, the Greater
676 Caribbean, the Amazon Plume and the Bay of Bengal. *Remote Sensing of Environment*,
677 235, 111469. https://doi.org/10.1016/j.rse.2019.111469

678 Liu, S., Ye, W., Chen, M. T., Pan, H. J., Cao, P., Zhang, H., Khokiattiwong, S., Kornkanitnang,
679 N., & Shi, X. (2021). Millennial-scale variability of Indian summer monsoon during the
680 last 42 kyr: Evidence based on foraminiferal Mg/Ca and oxygen isotope records from the
681 central Bay of Bengal. *Palaeogeography, Palaeoclimatology, Palaeoecology*, *562*,
682 110112. https://doi.org/10.1016/j.palaeo.2020.110112

683 Locarnini, M., Mishonov, A. V., Baranova, O. K., Boyer, T. P., Zweng, M. M., Garcia, H. E.,
684 Reagan, J. R., Seidov, D., Weathers K. W., Paver C. R., & Smolyar, I. (2018). World
685 ocean atlas 2018, volume 1: Temperature. https://archimer.ifremer.fr/doc/00651/76338/

686 Lombard, F., da Rocha, R. E., Bijma, J., & Gattuso, J. P. (2010). Effect of carbonate ion
687 concentration and irradiance on calcification in planktonic foraminifera. *Biogeosciences*,
688 7(1), 247-255. https://doi.org/10.5194/bg-7-247-2010

689 Lotliker, A. A., Omand, M. M., Lucas, A. J., Laney, S. R., Mahadevan, A., & Ravichandran, M.
690 (2016). Penetrative radiative flux in the Bay of Bengal. *Oceanography*, 29(2), 214-221.

691 Lukas, R., & Lindstrom, E. (1991). The mixed layer of the western equatorial Pacific Ocean.
692 *Journal of Geophysical Research*: Oceans, 96(S01), 3343-3357.
693 https://doi.org/10.1029/90JC01951

694 Madhu, N. V., Jyothibabu, R., Maheswaran, P. A., Gerson, V. J., Gopalakrishnan, T. C., & Nair,
695 K. K. C. (2006). Lack of seasonality in phytoplankton standing stock (chlorophyll a) and
696 production in the western Bay of Bengal. *Continental Shelf Research* 26, no. 16: 1868-
697 1883. https://doi.org/10.1016/j.csr.2006.06.004

698 Maeda, A., Kuroyanagi, A., Iguchi, A., Gaye, B., Rixen, T., Nishi, H., & Kawahata, H. (2022).
699 Seasonal variation of fluxes of planktic foraminiferal tests collected by a time-series
700 sediment trap in the central Bay of Bengal during three different years. *Deep Sea*
701 *Research Part I: Oceanographic Research Papers*, 103718.
702 https://doi.org/10.1016/j.dsr.2022.103718

Marchitto, T. M., Curry, W. B., Lynch-Stieglitz, J., Bryan, S. P., Cobb, K. M., & Lund, D. C. (2014). Improved oxygen isotope temperature calibrations for cosmopolitan benthic foraminifera. *Geochimica et Cosmochimica Acta*, 130, 1-11. https://doi.org/10.1016/j.gca.2013.12.034

Meilland, J., Siccha, M., Weinkauf, M. F., Jonkers, L., Morard, R., Baranowski, U., Baumeister, A., Bertlich, J., Brummer, G. J., Debray, P., Fritz-Endres, T., Groeneveld, J., Magerl, L., Munz, P., Rillo, M. C., Schmidt, C., Takagi, H., Theara, G., & Kučera, M. (2019). Highly replicated sampling reveals no diurnal vertical migration but stable species-specific vertical habitats in planktonic foraminifera. *Journal of Plankton Research*, 41(2), 127-141. https://doi.org/10.1093/plankt/fbz002

Mix, A. C. (1987). The oxygen-isotope record of glaciation. *The Geology of North America*, 3, 111-135. https://doi.org/10.1130/DNAG-GNA-K3.111

Mohtadi, M., Oppo, D. W., Lückge, A., DePol-Holz, R., Steinke, S., Groeneveld, J., Hemme, N., & Hebbeln, D. (2011). Reconstructing the thermal structure of the upper ocean: Insights from planktic foraminifera shell chemistry and alkenones in modern sediments of the tropical eastern Indian Ocean. *Paleoceanography*, 26(3). https://doi.org/10.1029/2011PA002132

Mulitza, S., Boltovskoy, D., Donner, B., Meggers, H., Paul, A., & Wefer, G. (2003). Temperature: $\delta^{18}O$ relationships of planktonic foraminifera collected from surface waters. *Palaeogeography, Palaeoclimatology, Palaeoecology*, 202(1-2), 143-152. https://doi.org/10.1016/S0031-0182(03)00633-3

Mulitza, S., Dürkoop, A., Hale, W., Wefer, G., & Stefan Niebler, H. (1997). Planktonic foraminifera as recorders of past surface-water stratification. *Geology*, 25(4), 335-338. https://doi.org/10.1130/0091-7613(1997)025<0335:PFAROP>2.3.CO;2

Mulitza, S., Wolff, T., Pätzold, J., Hale, W., & Wefer, G. (1998). Temperature sensitivity of planktic foraminifera and its influence on the oxygen isotope record. *Marine Micropaleontology*, 33(3-4), 223-240. https://doi.org/10.1016/S0377-8398(97)00040-6

Muraleedharan, K. R., Jasmine, P., Achuthankutty, C. T., Revichandran, C., Kumar, P. D., Anand, P., & Rejomon, G. (2007). Influence of basin-scale and mesoscale physical processes on biological productivity in the Bay of Bengal during the summer monsoon. *Progress in Oceanography*, 72(4), 364-383. https://doi.org/10.1016/j.pocean.2006.09.012

Naik, S. S., Divakar Naidu, P., Foster, G. L., & Martínez-Botí, M. A. (2015). Tracing the strength of the southwest monsoon using boron isotopes in the eastern Arabian Sea. *Geophysical Research Letters*, 42(5), 1450-1458. https://doi.org/10.1002/2015GL063089

Narvekar, J., & Kumar, S. P. (2006). Seasonal variability of the mixed layer in the central Bay of Bengal and associated changes in nutrients and chlorophyll. D*eep Sea Research Part I: Oceanographic Research Papers*, 53(5), 820-835. https://doi.org/10.1016/j.dsr.2006.01.012

Narvekar, J., & Kumar, S. P. (2014). Mixed layer variability and chlorophyll a biomass in the Bay of Bengal. *Biogeosciences*, 11(14), 3819-3843. https://doi.org/10.5194/bg-11-3819-2014

NASA Goddard Space Flight Center, Ocean Ecology Laboratory, Ocean Biology Processing Group. Moderate-resolution Imaging Spectroradiometer (MODIS) Aqua PAR Data; NASA OB.DAAC, Greenbelt, MD, USA. Accessed on 12/10/2020

Nilsson-Kerr, K., Anand, P., Sexton, P. F., Leng, M. J., & Naidu, P. D. (2022). Indian Summer Monsoon variability 140–70 thousand years ago based on multi-proxy records from the Bay of Bengal. *Quaternary Science Reviews*, 279, 107403. https://doi.org/10.1016/j.quascirev.2022.107403

Nürnberg, D., Bijma, J., & Hemleben, C. (1996). Assessing the reliability of magnesium in foraminiferal calcite as a proxy for water mass temperatures. *Geochimica et Cosmochimica Acta,* 60(5), 803-814. https://doi.org/10.1016/0016-7037(95)00446-7

Nürnberg, D., Müller, A., & Schneider, R. R. (2000). Paleo-sea surface temperature calculations in the equatorial east Atlantic from Mg/Ca ratios in planktic foraminifera: A comparison to sea surface temperature estimates from U37K′, oxygen isotopes, and foraminiferal transfer function. *Paleoceanography*, 15(1), 124-134. https://doi.org/10.1029/1999PA000370

Ota, Y., Kuroda, J., Yamaguchi, A., Suzuki, A., Araoka, D., Ishimura, T., NGHP Expedition 02 JAMSTEC Science Team, & Kawahata, H. (2019). Monsoon-influenced variations in plankton community structure and upper-water column stratification in the western Bay of Bengal during the past 80 ky. *Palaeogeography, Palaeoclimatology, Palaeoecology*, 521, 138-150. https://doi.org/10.1016/j.palaeo.2019.02.020

Ponton, C., Giosan, L., Eglinton, T. I., Fuller, D. Q., Johnson, J. E., Kumar, P., & Collett, T. S. (2012). Holocene aridification of India. *Geophysical Research Letters*, 39(3). https://doi.org/10.1029/2011GL050722

Peeters, F. J., & Brummer, G. J. A. (2002). The seasonal and vertical distribution of living planktic foraminifera in the NW Arabian Sea. *Geological Society, London, Special Publications*, 195(1), 463-497. https://doi.org/10.1144/GSL.SP.2002.195.01.

Piotrowski, A. M., Banakar, V. K., Scrivner, A. E., Elderfield, H., Galy, A., & Dennis, A. (2009). Indian Ocean circulation and productivity during the last glacial cycle. *Earth and Planetary Science Letters*, 285(1-2), 179-189. https://doi.org/10.1016/j.epsl.2009.06.007

Pracht, H., Metcalfe, B., & Peeters, F. J. (2019). Oxygen isotope composition of the final chamber of planktic foraminifera provides evidence of vertical migration and depth-integrated growth. *Biogeosciences*, 16(2), 643-661. https://doi.org/10.5194/bg-16-643-2019

Prasad, T. G. (1997). Annual and seasonal mean buoyancy fluxes for the tropical Indian Ocean. *Current Science*, 667-674.

Rao, R. R., & Sivakumar, R. (2003). Seasonal variability of sea surface salinity and salt budget of the mixed layer of the north Indian Ocean. *Journal of Geophysical Research: Oceans*, 108(C1), 9-1. https://doi.org/10.1029/2001JC000907

Rebotim, A., Voelker, A. H., Jonkers, L., Waniek, J. J., Meggers, H., Schiebel, R., Fraile, I., Schulz, M., & Kučera, M. (2017). Factors controlling the depth habitat of planktonic foraminifera in the subtropical eastern North Atlantic. *Biogeosciences*, 14(4), 827-859. https://doi.org/10.5194/bg-14-827-2017

Rixen, T., Gaye, B., Emeis, K.C., Ramaswamy, V., & Ittekkot, V. (2017): Particle fluxes obtained from sediment trap experiments in the northern Indian Ocean. PANGAEA. https://doi.org/10.1594/PANGAEA.879702

Saito, T., Thompson, P. R., & Breger, D. (1981). Systematic index of Recent and Pleistocene planktonic foraminifera. *University of Tokyo Press*.

Sarma, V. V. S. S., Chopra, M., Rao, D. N., Priya, M. M. R., Rajula, G. R., Lakshmi, D. S. R., & Rao, V. D. (2020a). Role of eddies on controlling total and size-fractionated primary production in the Bay of Bengal. *Continental Shelf Research,* 204, 104186. https://doi.org/10.1016/j.csr.2020.104186

Sarma, V. V. S. S., Sridevi, B., Maneesha, K., Sridevi, T., Naidu, S. A., Prasad, V. R., Venkataramana, V., Acharya, T., Bharati, M. D., Subbaiah, Ch. V., Kiran, B. S., Reddy, N. P. C., Sarma, V. V., Sadhuram Y., & Murty, T. V. R. (2013). Impact of atmospheric and physical forcings on biogeochemical cycling of dissolved oxygen and nutrients in the coastal Bay of Bengal. *Journal of oceanography*, 609(2), 229-243. https://doi.org/10.1007/s10872-012-0168-y

Sarma, V. V. S. S., Vivek, R., Rao, D. N., & Ghosh, V. R. D. (2020b). Severe phosphate limitation on nitrogen fixation in the Bay of Bengal. *Continental Shelf Research*, 205, 104199. https://doi.org/10.1016/j.csr.2020.104199

Schiebel, R., & Hemleben, C. (2017). Planktic foraminifers in the modern ocean (pp. 1-358). Berlin: Springer.

Shenoi, S. S. C., Shankar, D., & Shetye, S. R. (2002). Differences in heat budgets of the near - surface Arabian Sea and Bay of Bengal: Implications for the summer monsoon. *Journal of Geophysical Research: Oceans*, 107(C6), 5-1. https://doi.org/10.1029/2000JC000679

Sijinkumar, A. V., Clemens, S., Nath, B. N., Prell, W., Benshila, R., & Lengaigne, M. (2016). $\delta^{18}O$ and salinity variability from the Last Glacial Maximum to Recent in the Bay of Bengal and Andaman Sea. *Quaternary Science Reviews*, 135, 79-91. https://doi.org/10.1016/j.quascirev.2016.01.022

Singh, A., Gandhi, N., Ramesh, R., & Prakash, S. (2015). Role of cyclonic eddy in enhancing primary and new production in the Bay of Bengal. *Journal of Sea Research*, 97, 5-13. https://doi.org/10.1016/j.seares.2014.12.002

Spero, H. J., & Lea, D. W. (1993). Intraspecific stable isotope variability in the planktic foraminifera *Globigerinoides sacculifer*: Results from laboratory experiments. *Marine Micropaleontology*, 22(3), 221-234. https://doi.org/10.1016/0377-8398(93)90045-Y

Spero, H. J., & Parker, S. L. (1985). Photosynthesis in the symbiotic planktonic foraminifer Orbulina universa, and its potential contribution to oceanic primary productivity. *The Journal of Foraminiferal Research*, 15(4), 273-281. https://doi.org/10.2113/gsjfr.15.4.273

Stainbank, S., Kroon, D., Rüggeberg, A., Raddatz, J., de Leau, E. S., Zhang, M., & Spezzaferri, S. (2019). Controls on planktonic foraminifera apparent calcification depths for the northern equatorial Indian Ocean. *PloS one,* 14(9), e0222299. https://doi.org/10.1371/journal.pone.0222299

827 Steph, S., Regenberg, M., Tiedemann, R., Mulitza, S., & Nürnberg, D. (2009). Stable isotopes of
828 planktonic foraminifera from tropical Atlantic/Caribbean core-tops: Implications for
829 reconstructing upper ocean stratification. *Marine Micropaleontology*, 71(1-2), 1-19.
830 https://doi.org/10.1016/j.marmicro.2008.12.004

831 Stoll, H. M., Arevalos, A., Burke, A., Ziveri, P., Mortyn, G., Shimizu, N., & Unger, D. (2007).
832 Seasonal cycles in biogenic production and export in Northern Bay of Bengal sediment
833 traps. *Deep Sea Research Part II: Topical Studies in Oceanography* 54, no. 5-7: 558-580.
834 https://doi.org/10.1016/j.dsr2.2007.01.002

835 Sun, C. & Co-Authors (2010). The Data Management System for the Global Temperature and
836 Salinity Profile Programme in Proceedings of OceanObs.09: Sustained Ocean
837 Observations and Information for Society (Vol. 2), Venice, Italy, 21-25 September 2009,
838 Hall, J., Harrison, D.E. & Stammer, D., Eds., ESA Publication WPP-306,
839 doi:10.5270/OceanObs09.cwp.86

840 Subha Anand, S., Rengarajan, R., Sarma, V. V. S. S., Sudheer, A. K., Bhushan, R., & Singh, S.
841 K. (2017). Spatial variability of upper ocean POC export in the Bay of Bengal and the
842 Indian Ocean determined using particle-reactive ^{234}Th. *Journal of Geophysical Research:*
843 *Oceans*, 122(5), 3753-3770. https://doi.org/10.1002/2016JC012639

844 Takagi, H., Kimoto, K., Fujiki, T., Saito, H., Schmidt, C., Kučera, M., & Moriya, K. (2019).
845 Characterizing photosymbiosis in modern planktonic foraminifera. *Biogeosciences*,
846 16(17). https://doi.org/10.5194/bg-16-3377-2019

847 Takagi, H., Moriya, K., Ishimura, T., Suzuki, A., Kawahata, H., & Hirano, H. (2015). Exploring
848 photosymbiotic ecology of planktic foraminifers from chamber-by-chamber isotopic
849 history of individual foraminifers. *Paleobiology*, 41(1), 108-121.
850 https://doi.org/10.1017/pab.2014.7

851 Tedesco, K., Thunell, R., Astor, Y., & Muller-Karger, F. (2007). The oxygen isotope
852 composition of planktonic foraminifera from the Cariaco Basin, Venezuela: Seasonal and
853 interannual variations. *Marine Micropaleontology*, 62(3), 180-193.
854 https://doi.org/10.1016/j.marmicro.2006.08.002

855 Thadathil, P., Muraleedharan, P. M., Rao, R. R., Somayajulu, Y. K., Reddy, G. V., &
856 Revichandran, C. (2007). Observed seasonal variability of barrier layer in the Bay of
857 Bengal. *Journal of Geophysical Research: Oceans*, 112(C2).
858 https://doi.org/10.1029/2006JC003651

859 Tripati, A. K., Delaney, M. L., Zachos, J. C., Anderson, L. D., Kelly, D. C., & Elderfield, H.
860 (2003). Tropical sea-surface temperature reconstruction for the early Paleogene using
861 Mg/Ca ratios of planktonic foraminifera. *Paleoceanography* 18, no. 4.
862 https://doi.org/10.1029/2003PA000937

863 Unger, D., Ittekkot, V., Schäfer, P., Tiemann, J., & Reschke, S. (2003). Seasonality and
864 interannual variability of particle fluxes to the deep Bay of Bengal: influence of riverine
865 input and oceanographic processes. *Deep Sea Research Part II: Topical Studies in*
866 *Oceanography*, 50(5), 897-923. https://doi.org/10.1016/S0967-0645(02)00612-4

867 Venancio, I. M., Belem, A. L., Santos, T. P., Lessa, D. O., Albuquerque, A. L. S., Mulitza, S.,
868 Schulz, M., & Kučera, M. (2017). Calcification depths of planktonic foraminifera from

the southwestern Atlantic derived from oxygen isotope analyses of sediment trap material. *Marine Micropaleontology*, 136, 37-50. https://doi.org/10.1016/j.marmicro.2017.08.006

Vinayachandran, P. N. (2009). Impact of physical processes on chlorophyll distribution in the Bay of Bengal. *Indian Ocean Biogeochemical Processes and Ecological Variability*, 185, 71-86. https://doi.org/10.1029/2008GM000705

Vinayachandran, P. N., & Mathew, S. (2003). Phytoplankton bloom in the Bay of Bengal during the northeast monsoon and its intensification by cyclones. *Geophysical Research Letters* 30, no. 11. https://doi.org/10.1029/2002GL016717

Vinayachandran, P.N., McCreary Jr, J.P., Hood, R.R., & Kohler, K.E. (2005). A numerical investigation of the phytoplankton bloom in the Bay of Bengal during Northeast Monsoon. *Journal of Geophysical Research: Oceans*, 110(C12). https://doi.org/10.1029/2005JC002966

Wejnert, K. E., Thunell, R. C., & Astor, Y. (2013). Comparison of species-specific oxygen isotope paleotemperature equations: Sensitivity analysis using planktonic foraminifera from the Cariaco Basin, Venezuela. *Marine Micropaleontology,* 101, 76-88. https://doi.org/10.1016/j.marmicro.2013.03.001

Williams, D. F., & Healy-Williams, N. (1980). Oxygen isotopic-hydrographic relationships among recent planktonic foraminifera from the Indian Ocean. *Nature*, 283(5750), 848-852. https://doi.org/10.1038/283848a0

Wycech, J. B., Kelly, D. C., Kitajima, K., Kozdon, R., Orland, I. J., & Valley, J. W. (2018). Combined effects of gametogenic calcification and dissolution on $\delta^{18}O$ measurements of the planktic foraminifer *Trilobatus sacculifer*. *Geochemistry, Geophysics, Geosystems*, 19(11), 4487-4501. https://doi.org/10.1029/2018GC007908

Yang, H., & Wang, F. (2009). Revisiting the thermocline depth in the equatorial Pacific. *Journal of climate*, 22(13), 3856-3863. https://doi.org/10.1175/2009JCLI2836.1

Zweng, M. M., Seidov, D., Boyer, T., Locarnini, M., Garcia, H., Mishonov, A., Baranova O. K., Weathers, K. W., Paver, C. R., & Smolyar, I. (2019). World ocean atlas 2018, volume 2: Salinity.